Egyptian Journal of Radiology and Nuclear Medicine

REVIEW

Open Access

Assessment of intravoxel incoherent motion MR imaging for differential diagnosis of breast lesions and evaluation of response: a systematic review

Mohannad Ahmed Sahib[1], Arian Arvin[2*], Nasrin Ahmadinejad[3], Raad Ajeel Bustan[1] and Hussein Abed Dakhil[1]

Abstract

Background: The current study aimed to assess the performance for quantitative differentiation and evaluation of response in categorized observations from intravoxel incoherent motion analyses of patients based on breast tumors. To assess the presence of heterogeneity, the Cochran's *Q* tests for heterogeneity with a significance level of $P < 0.1$ and I^2 statistic with values > 75% were used. A random-effects meta-analysis model was used to estimate pooled sensitivity and specificity. The standardized mean difference (SMD) and 95% confidence intervals of the true diffusivity (D), pseudo-diffusivity (*D**), perfusion fraction (*f*) and apparent diffusion coefficient (ADC) were calculated, and publication bias was evaluated using the Begg's and Egger's tests and also funnel plot. Data were analyzed by STATA v 16 (StataCorp, College Station).

Results: The pooled *D* value demonstrated good measurement performance showed a sensitivity 86%, specificity 86%, and AUC 0.91 (SMD − 1.50, $P < 0.001$) in the differential diagnosis of breast lesions, which was comparable to that of the ADC that showed a sensitivity of 76%, specificity 79%, and AUC 0.85 (SMD 1.34, $P = 0.01$), then by the *f* it showed a sensitivity 80%, specificity 76%, and AUC 0.85 (SMD 0.89, $P = 0.001$), and *D** showed a sensitivity 84%, specificity 59%, and AUC 0.71 (SMD − 0.30, $P = 0.20$).

Conclusion: The estimated sensitivity and specificity in the current meta-analysis were acceptable. So, this approach can be used as a suitable method in the differentiation and evaluation response of breast tumors.

Keywords: Intravoxel incoherent motion (IVIM), Quantitative of breast tumors, Diffusion-weighted imaging (DWI), Evaluation of response, Meta-analysis

Background

As a common health problem of women, breast cancer (BC) has various histological types and therapeutic approaches [1–3]. Hence, determining the subtype of the disease is of high value [4, 5]. Gene expression profiling is a useful method to achieve this purpose. Nevertheless, gene expression is not always feasible and the following options have been used for BC subtypes evaluation: estrogen receptor (ER), progesterone receptor (PR), human epidermal growth factor receptor 2 (HER2), and Ki-67 labeling indexes using immunohistochemical techniques. In such cases, tissue biopsy can be used to obtain valuable information; however, it may cause stress and suffering for patients. Hence, differentiation between different subtypes of the tumor using noninvasive methods would be useful [6, 7]. Therefore, one of the commonly applied methods to diagnose BC is mammography. While its sensitivity to diagnose dense breast tissue is low, it has good sensitivity for fatty tissue [8]. Due

*Correspondence: aryana@sina.tums.ac.ir
[2] Radiology-TUMS (Cancer Institute-ADIR), Tehran University of Medical Sciences (TUMS), Tehran, Iran
Full list of author information is available at the end of the article

to several reasons, including low cost and being convenient, the application of ultrasound (US) to detect BC is on the rise [9]. However, it should be noted that detection of nonmass BC is difficult in this method.

As a noninvasive technique, magnetic resonance imaging (MRI) is an appropriate radiological method to evaluate BC [10]. According to the literature, diffusion-weighted imaging (DWI) can effectively reflect tumor cellularity and tissue organization [11–13]. Due to enhanced cellularity that causes restricted water molecule movement, which roots in decreased extracellular space, diffusion in malignant tumors is restricted. This issue has resulted in an increasing inclination towards using the apparent diffusion coefficient (ADC) to evaluate cellularity [14–19].

Intravoxel incoherent motion (IVIM) is a valued imaging technique capable of differentiation between diffusion via a biexponential model analysis based on multiple *b*-values [20, 21]. In this line, Le Bihan and colleagues [21] developed a technique for IVIM that its effects on microcapillary perfusion are proved by some studies using DWI [22–25]. In cases that several *b*-values (usually ranging from 0 to 1500 s/mm^2 for body imaging) are applied in DWI, the signal intensity at low *b*-values (0–200 s/mm^2) indicates microcirculation within capillaries. In the same way, the higher the b value (> 200 s/mm^2), the better the signal intensity reflects tissue diffusivity [24, 26]. The IVIM technique can provide different quantitative parameters, such as slow ADC, fast ADC, and a fraction of fast ADC values that show the perfusion and diffusion of the tissues. It should be considered that DWI cannot remove the effect of microcirculation. As the slow ADC value removes the impact of blood perfusion, it can show the true diffuse state of water molecules, which, as compared to values obtained using ADC, are more accurate.

Heterogeneity is a prominent characteristic of cancer that negatively affects treatment strategy [27, 28], which is also true for BC [29]. Hence, quantitative analysis of tumor heterogeneity using IVIM parameters and determining their correlation with BC histological characteristics would be of high use. It has been proven that IVIM metrics not only can differentiate malignant and benign lesions [23, 30, 31] but also can determine the correlation between a BC subtype and IVIM factors [25, 32–34]. In addition, these metrics can be used to predict the neoadjuvant therapeutic response in cases with BC [37]. Therefore, the current meta-analysis aimed to summarize the available knowledge on intravoxel incoherent motion techniques for quantitative differentiation and response evaluation after neoadjuvant chemotherapy in BC. Besides, the IVIM is potentially able to replace dynamic contrast MRI, so that avoid the cost and side effects of contrast media and improve the diagnostic performance of MRI in patients.

Methods

Search strategy

A meta-analysis search using PubMed (https://pubmed.ncbi.nlm.nih.gov), Embase (https://www.embase.com), Web of Science (https://apps.webofknowledge com), SEMANTIC SCHOLAR, Google Scholar, PROQUEST, and Cochrane Library databases (https://www.cochranelibrary.com) were performed independently by three radiologists to identify articles published before February 2021, using the keywords “breast cancer.” "Intravoxel Incoherent Motion" AND "biexponential" AND "MRI OR magnetic resonance imaging" AND "diffusion-weighted imaging OR DWI" AND "Neoadjuvant Chemotherapy OR NACT" AND "monitoring and response" AND "Breast or Breast Neoplasms, Ductal, Breast or Breast Neoplasms or Breast Diseases or Breast Carcinoma In Situ or Breast Cancer".

Study selection and data extraction

The three radiologists reviewed all 680 abstracts after duplication removal and subsequently the full text of the 90 articles was obtained if the following inclusion criteria were fulfilled: (1) included the diagnostic accuracy of breast lesions underwent diagnostic IVIM-DWI; (2) constituted original research rather than a meta-analysis, a review article, case report or case series; (3) published in English; (4) results are from humans and not animals; (5) included breast lesions IVIM-MRI protocol; (6) included sufficient data, with > 20 patients to calculate true positive (TP), false positive (FP), false negative (FN) and true negative (TN) for constructing a 2×2 contingency table; and (7) patients at high risk of breast lesions using pathological analysis (surgical resection, explant and/or biopsy) or imaging from follow-up corresponding to the guidelines for the standardization of breast imaging, diagnosis, classification and reporting of breast carcinoma. In addition, articles from the same institution, which involved an overlap period of patient recruitment, were considered to have an overlapping population. In these cases, the study which had the larger number of BC cases was included. A total of 590 studies were excluded according to the following exclusion criteria: (1) they were not relevant to the present meta-analysis if they fit one of the followings conditions: cancer type involves cancer other than BC; (2) they evaluated previously treated BC; (3) the sensitivity and specificity were not evaluated; (4) there was a lack of sufficient data to construct a 2×2 contingency table; and (5) there was study population overlap. A total of 16 studies were included for analysis. In addition, the reference list of these 16 studies was reviewed (Fig. 1).

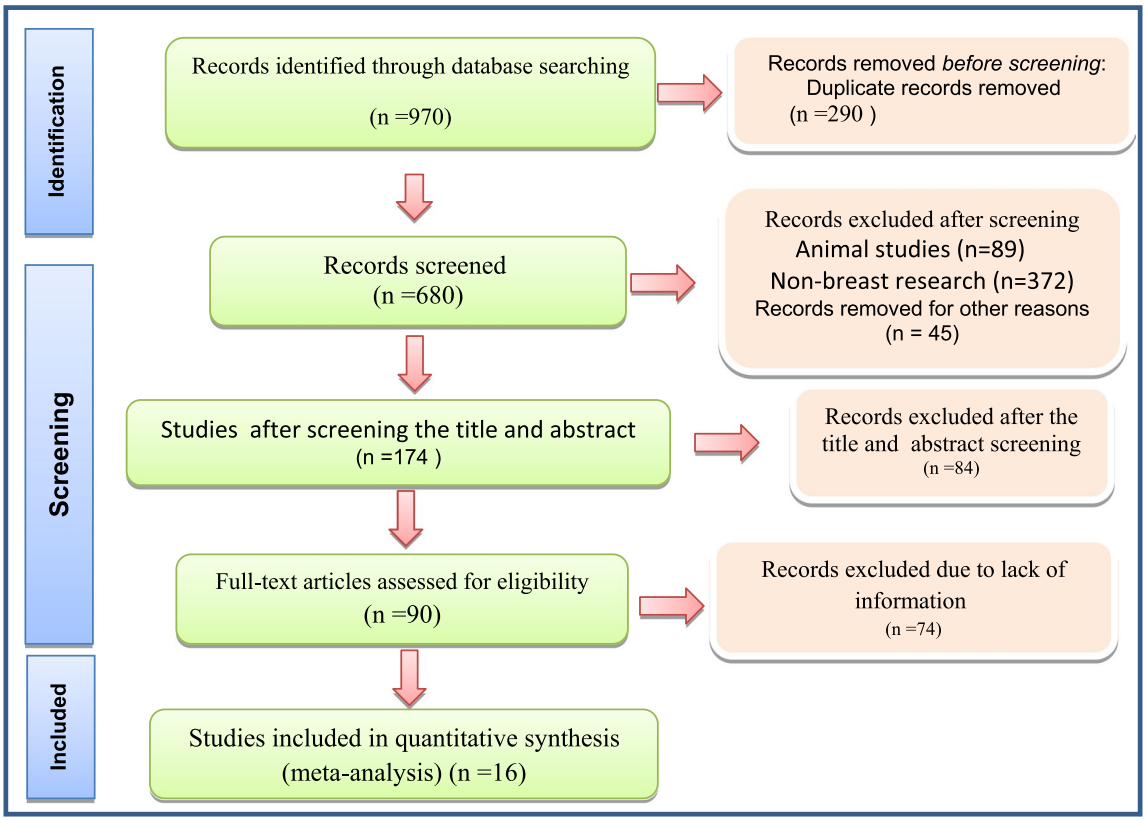

Fig. 1 PRISMA flow diagram for included studies in the current meta-analysis

Quality and risk of bias assessment

The Quality Assessment of Diagnostic Accuracy Studies (QUADAS) was used to assess the quality and risk of bias in included studies. No studies were excluded due to poor quality [63].

Statistical analysis

To assess the presence of heterogeneity, the Cochran's Q tests for heterogeneity with a significance level of $P<0.1$ and I^2 statistic with values > 75% to the presence of heterogeneity were used. Due to the presence of significant heterogeneity, a random-effects model with 95% CI was used to estimate pooled sensitivity and specificity. To assess the effect of sample size and study year on the heterogeneity of pooled estimations, the simple meta-regression model was used. Publication bias was evaluated using the Begg's and Egger's tests and funnel plot. Data were analyzed by STATA v 11 (StataCorp, College Station, TX, USA).

Results

We obtained 16 related papers through the electronic databases of Medline/PubMed and Science Direct from 2014 to 2021 for studies that reported the percentage of observations was confirmed as breast lesions. We excluded studies that included some papers because of a lack of necessary criteria for patients or methodology. A summary of the details of all included studies is tabulated in Tables 1, 2 and 3.

Measurement of ADC value used for of breast tumor

Eight papers about ADC used in distinguishing breast lesions were involved for investigation. The $\chi^2=31.73$, $P<0.001$ of the heterogeneity test ($I^2=78\%$) was proposed in height heterogeneity between the comprised papers. The plot in Fig. 2 demonstrates the apportionment of the ADC between breast lesions. A random effects pattern made an SMD of -1.38 $(-1.76, -1.00)$ $(P<0.001)$ between breast tumor for ADC. The Begg's test proposed no publication bias linking to the ADC $(P=0.428)$.

Measurement of *D* value used for of breast tumor

Ten papers about D used in distinguishing breast lesions were involved for investigation. The $\chi^2=37.49$ and $P<0.001$ of the heterogeneity test ($I^2=76\%$) was proposed in height heterogeneity between the comprised papers. The plot in Fig. 3 demonstrates the apportionment of the

Table 1 Overview of studies included

Author	Year	SD (P/R)	Pat. no	Age: median (range)	Machine type	Parameters	*b*-values (s/mm^2)	Tumor diameters (mm)	Malignant	Benign	Main findings
Suo et al. [35]	2021	**R**	144	51.7 ± 11.8	3-T Philip	ADC, DDC, *D**, *f*	0, 10, 30, 50, 100, 150, 200, 500, 800, 1000, 1500, 2000, and 2500	39.8 ± 21.2	NA	NA	Indifferent ADC change at after treatment was a predictor of pCR pre NAC in BC
Kim et al. [36]	2018	R	46	45 (25–67)	3-T	ADC, *D*, *D**, *f*	0, 25, 50, 75, 100, 150, 200, 300, 500 and 800	4.15 (2.2–9.3)	NA	NA	D & ADC are suitable for the calculation of response to NAC in BC patients
Cho et al. [37]	2017	R	31	47.40 (28–66)	1.5 or 3 T	ADC, *D*, *D**, *f*, VTT%	0, 30, 60, 90, 120, 250, 400, 600, 800, 1000	13.84 (3.43, 44.45)	NA	NA	*D* value displayed predictive capabilities; measured and heterogeneous *D** bid poor prognosis. Baseline ADC&D values were not important interpreters of response
Che et al. [38]	2016	P	36	50.9 (27–75)	3.0 T	*D*, *D**, *f*, MD, *V*	0, 10, 20, 30, 50, 70, 100, 150, 200, 400, 800, and 1000	4.89–1.52	NA	NA	IVIM factors, particularly the *D* and *f* value, displayed likely value in the before-treatment prediction & early response checking to NAC in BC
Bedair et al. [39]	2017	P	36	55 (32–75)	3.0-T	ADC, DDC, and Dt	0, 30, 60, 90, 120, 300, 600, 900	1.2–12	NA	NA	DW is sensitive to baseline and early usage vicissitudes in BC by bi-exponential
He et al. [40]	**2021**	**P**	202	43.8 ± 9.2	3 T Siemens	ADC, *D*, *D**, *f*, MK, and MD	0, 30, 50, 80, 120, 160, 200, 500, 1000, 1500, 2000	**NA**	152	63	ADC was improved than that of *D** and there was no numerical change among *D* and MD. There was no significant change in investigative efficiency among ADC alone as related to ADC & MK
Meng et al. [41]	**2020**	**P**	121	57 ± 11	3 T GE	*D*, *D**, *f*	0, 50, 75, 100, 150, 200, 400, 800, 1000	Malignant: 25.6 ± 11.4; Benign: 22.4 ± 8.9	65	58	IVIM-parameter *f*, *D**, and *D* standards displayed associations with some predictive features for BC

Table 1 (continued)

Author	Year	SD (P/R)	Pat. no	Age: median (range)	Machine type	Parameters	*b*-values (s/mm^2)	Tumor diameters (mm)	Malignant	Benign	Main findings
Song et al. [42]	2018	**R**	85	54	3 T Siemens	*D*, *D**, *f*	0, 10, 20, 30, 50, 70, 100, 150, 200, 400, 600, 1000	18 (8–48)	85	0	Showing the possibility of IVIM biomarkers to offer info on the biotic and kinematic possessions of BC devoid of a contrast agent
Zhao et al. [43]	**2018**	**R**	141	50.2 ± 10.5	3 T GE		0, 50, 100, 150, 200, 400, 500, 1000, 1500	NA	119	22	The IVIM biomarkers of cancer, tumor superiority and per tumor tissues in many subtypes of BC may perhaps be suitable for difference of BC subtypes and to evaluate the invasive amount of the tumors
Mao [44]	2018	**R**	124	45.3 ± 8.7	3 T Siemens	*D*, *D**, *f*	0, 50, 100, 150, 200, 250, 300, 400, 600, 800, 1000, 1200	**NA**	77	47	IVIM canister advantage to increase the specificity & accuracy in difference identification of breast benign & malignant lesions
Lin et al. [45]	**2017**	**P**	**93**	48	3 T Philips	**ADC,** *D*, *D**, *f*	0, 50, 100, 150, 200, 500, 800	**NA**	51	47	IVIM offers measurable quantity of cellularity & vascularity for describing BC. In *D* displays moral potential for classifying BC
Iima et al. [46]	**2017**	**P**	199	58.5 (20–88)	3 T Siemens	**ADC,** *D*, *D**, *f*	5, 10, 20, 30, 50, 70, 100, 200, 400, 600, 800, 1000, 1500, 2000, 2500	Benign: 25.7 (10–100); Malignant: 18.2 (10–62)	152	47	IVIM & non-Gaussian diffusion factors, & their mishmash through integrated diagnostic approaches, may provide BC investigative accuracy like to BI-RADS devoid of the necessity for contrast agents

Table 1 (continued)

Author	Year	SD (P/R)	Pat. no	Age: median (range)	Machine type	Parameters	*b*-values (s/mm^2)	Tumor diameters (mm)	Malignant	Benign	Main findings
Cho et al. [47]	**2016**	**R**	**62**	48.44 ± 11.14	3 T Siemens	**ADC,** *D*, *D**, *f*	0, 30, 70, 100, 150, 200, 300, 400, 500, 800	32.5 ± 27.2	**50**	**12**	Innovative DWI display relations by molecular predictive aspects & BC. This study illuminate certain of the practical variability in usage response between BC patients
Wang et al. [48]	2016	**R**	48	46.85 ± 8.63	3 T GE	**ADC,** *D*, *D**, *f*	0, 10, 20, 50, 100, 200, 300, 400, 600, 800	Malignant: 159.9 (82.6–243.2) mm^2; Benign: 87.5	31	23	*D* can efficiently accompaniment current predictable DW &DCE in distinguishing malignant since benign BC. IVIM united with DCE is a forceful incomes of assessing BC
Liu et al. [49]	**2016**	**P**	**56**	**NA**	1.5 T Philips	**ADC,** *D*, *D**, *f*, Ktrans, Kep, Ve and Vp	0, 10, 20, 30, 50, 70, 100, 150, 200, 400, 600, 1000	Malignant: 28.32 ± 4.25; Benign: 22.27 ± 3.96	36	**23**	IVIM is suitable in the difference of BC. Important associations were found among perfusion parameters as of DCE &IVIM. IVIM may be a suitable adjunctive instrument to standard MRI in detecting BC
Bokacheva et al. [50]	2014	**R**	35	**57**	3 T GE	**ADC,** *D*, *D**, *f*	0, 30, 60, 90, 120, 400, 600, 800, 1000	Benign: 20 (8–48); Malignant: 38 (9–80)	26	**14**	The IVIM biomark offer exact documentation of malignant lesions

Bold values indicates the features of included studies in the current meta-analysis

D between breast tumor. A random-effects pattern made an SMD of −1.50 (−1.85, −1.14) ($P<0.001$) between breast tumor for *D*. The Begg's test proposed no publication bias linking to *D* ($P=0.112$).

Measurement of *D** value used for of breast tumor

Twelve papers about *D** used in distinguishing breast lesions were involved for investigation. The $\chi^2=123.02$ and $P<0.001$ of the heterogeneity test ($I^2=91\%$) was proposed in height heterogeneity between the comprised papers. The plot in Fig. 4 demonstrates the apportionment of the *D** between breast tumor. A random-effects pattern made an SMD of −0.30 (−0.76, 0.16) ($P=0.20$) between breast tumor for *D**. The Begg's test proposed no publication bias linking to *D** ($P=0.208$).

Measurement of *f** value used for of breast tumor

Twelve papers about *f* used in distinguishing breast lesions were involved for investigation. The $\chi^2=20.07$ and $P<0.04$ of the heterogeneity test ($I^2=45\%$) was proposed in height heterogeneity between the comprised papers. The plot in Fig. 5 demonstrates the apportionment of the *D** between breast tumor. A random-effects pattern made an SMD of 0.89 (0.75, 1.02) ($P<0.001$) between breast tumor for *f*. The Begg's test proposed no publication bias linking to *f* ($P=0.880$).

Measurement performance

The measurement performance as evaluated by pooling sensitivity, specificity, the ADC, *D*, *D**, and *f* values is recorded in Table 4. The *D* value demonstrated good measurement performance showed a sensitivity 86%, specificity 86%, and AUC 0.91 in the differential diagnosis of breast lesions, which was comparable to that of the ADC that showed a sensitivity of 76%, specificity 79%, and AUC 0.85, then by the *f* it showed a sensitivity 80%, specificity 76%, and AUC 0.85, and *D** showed a sensitivity 84%, specificity 59%, and AUC 0.71.

Meta-regression

To identify the cause of heterogeneity between studies, the effect of variables like years of study and sample size of different studies on pooled sensitivity and specificity was assessed. The effect of the year of study (*P*: 0.80) and sample size on heterogeneity between studies in the estimation of pooled sensitivity was not statistically significant (*P*: 0.49). Also, the effect of the year of study (*P*: 0.17) and sample size on heterogeneity between studies in the estimation of pooled specificity was not statistically significant (*P*: 0.72). The distribution of sensitivity and specificity according to different sample sizes is shown in Fig. 6.

Publication bias

According to the results of Begg's and Egger's test, there was a significant publication bias about the reported sensitivity (Begg's test *P*: 0.001, and Egger's test *P*: 0.001). Also according to the results of Begg's and Egger's test, there was a significant publication bias about the reported specificity (Begg's test $P<0.001$, and Egger's test $P<0.001$) (Fig. 7).

Quantitative analysis evaluation of response

The performance of IVIM in the prediction of the therapy response (mainly neoadjuvant chemotherapy [NAC]) in BC has been recently explored. Cho and colleagues found that the pretreatment average, skewness, and K of Dp were significant differentiators of responders from nonresponders in 32 lesions [37]. Kim and colleagues assessed 46 cases with stage II or III BC and found that pretreatment IVIM histogram parameters, including the mean, 25th percentile, 50th percentile, and 75th percentile of *D* obtained from the histogram of the whole tumor (Dmean, D25, D50, and D75, respectively), were significantly higher in good responders than in poorer responders [36]. Che et al. showed that the *f* value before NAC of patients with a pathologic complete response (pCR) was significantly larger than that of non-pCR patients and the change in *f* after two cycles of NAC were also significantly larger than that in the non-pCR group in 28 patients with locally advanced breast cancer [38]. These IVIM values and histogram metrics might serve as prognostic biomarkers for the selection of neoadjuvant treatment.

In three articles on IVIM as an MRI parameter, there were pre-treatment differences among responders and nonresponders. Bedair et al. [39] reported that prior to NAC, nonresponders had a higher mean Dt than responders ($0.85\pm0.05\times10^{-3}$mm^2/s and $1.02\pm0.05\times10^{-3}$mm^2/s, respectively) ($P=0.02$). In addition, responders had a better function concerning the *f* fraction, which was not statistically significant ($P=0.09$). Also, the *f* was significantly lower in nonresponders of the TNBC subtype ($12.4\pm4.1\%$ vs. $10.9\pm1.2\%$, $P=0.01$). Following NAC, enhanced mean values in *Dt* were not associated with a significant difference between response groups (36% vs. 23%, $P=0.14$). Moreover, decreased *f* fraction in responders (29%) was considerably different from the increase found in *f* in pNCR (5%, $P=0.05$). Che et al. found similar results [38]. At the mid-treatment period, the *D* presented excellent diagnostic prediction performance by the area of the curve 0.851 (95% CI 0.666–0.956), which is a bit higher than the *D** value (AUC = 0.579, 95% CI 0.379–0.762, $P=0.025$). Nevertheless, the *f* value presented an acceptable diagnostic performance (AUC = 0.772, 95% CI

Table 2 Findings regarding the response prediction pre and post-therapy based on the IVIM factors value and tumor size

Author	Year	IVIM mean ($\times 10^{-3}$ mm^2/s) or % change												Tumor size			*P* value
		Pre-NAC						Post-NAC						Before NAC (cm)	After NAC%Change (cm)		
		Response or Baseline			Nonresponse			Response			Nonresponse						
		D	*D**	*F*	*D*	*D**	*F*	*D*	*D**	*F*	*D*	*D**	*f*				
Suo et al. [35]	2021	1.00 ± 0.83	15.62 ± 4.18	9.27 ± 3.66	0.98 ± 0.80	15.44 ± 3.70	9.27 ± 2.98	0.78 ± 0.68	− 3.06 ± 6.36	1.78 ± 4.33	0.25 ± 0.35	− 1.97 ± 6.35	0.82 ± 3.86	39.8 ± 21.2	NA	− 34.0 ± 18.9	0.009
Kim et al. [36]	2018	1.22	5.87	45.17	1.10	7.33	43.33	1.37↑	6.04↑	49.56↑	1.15↑	6.58↓	45.23↑	4.15 (2.2–9.3)	3.05 (1.1–7.8)	− 20.22 (− 54.9–4.4)	0.023
Cho et al. [37]	2017	1.02	25.05	8.8	NA	NA	NA	0.99↓	25.54↑	8.7↓	1.05↑	17.16↓	11.7↑	13.84 (3.43, 44.45)	13.80 (3.43, 37.00)	− 40.2%	0.452
Che et al. [38]	2016	0.92	10.10	32.40	0.83	9.40	24.40	1.36 ± 0.30↑	8.98↓	14.51 ± 7.25↓	0.98 ± 0.23↑	20.00↑	20.69 ± 5.10↓	4.89–1.52	2.57 (2.03, 4.16)	− 39.2%	< 0.001
Bedair et al. [39]	2017	0.85 ± 0.05	NA	12.10 ± 2.02	1.02 ± 0.05	NA	10.32 ± 1.15	1.30 ± 0.14 (↑36%)	NA	8.48 ± 1.54 (↓29%)	1.28 ± 0.15 (↑23%)	NA	10.53 ± 2.51 (↑5%)	1.2–12	4.1 ± 0.4	1.5 ± 0.2	0.14

Table 3 The estimated sensitivity and specificity in the included studies in the current meta-analysis

	Author	Year	Threshold	AUC	Sensitivity	Specificity	TP	FP	FN	TN
ADC	He et al. [40]	2021	< 0.983	0.915	91.45%	82.54%	NA	NA	NA	NA
	Zhao et al. [43]	2018	1.15	0.9	0.857	0.893	63	2	17	20
	Lin et al. [45]	2017	1.203	0.931	0.894	0.843	46	5	7	40
	Cho et al. [47]	2015	NA	0.69	0.58	0.833	29	2	21	10
	Wang et al. [48]	2016	NA	NA	0.808	0.677	46	14	11	30
	Bokacheva et al. [50]	2014	1.54	0.72	0.65	0.71	17	4	9	10
D	Muzhen He et al. [40]	2021	< 0.952	0.909	90.13%	80.95%	NA	NA	NA	NA
	Meng et al. [41]	2020	1.01	0.809	0.7385	0.9138	48	5	17	53
	Zhao et al. [43]	2018	1.09	0.92	0.929	0.88	11	3	8	19
	Xijin Mao et al. [44]	2018	1.21	0.883	83.0	57.4	NA	NA	NA	NA
	Lin et al. [45]	2017	1.096	0.945	0.872	0.843	44	7	7	40
	Cho et al. [47]	2015	NA	0.77	0.66	0.917	33	1	17	11
	Wang et al. [48]	2016	NA	NA	0.937	0.874	53	6	4	38
	Liu et al. [49]	2016	1.02	0.917	0.89	0.83	32	4	4	19
	Bokacheva et al. [50]	2014	1.52	0.75	0.85	0.64	22	5	4	9
*D**	He [40]	2021	> 0.873	0.574	42.76%	77.78%	NA	NA	NA	NA
	Meng et al. [41]	2020	26.58	0.67	0.7385	0.547	85	10	34	12
	Zhao et al. [43]	2018	43.18	0.674	0.714	0.86	19	2	7	12
	Lin et al. [45]	2017	99.056	0.682	0.702	0.588	36	19	15	28
	Cho et al. [47]	2015	NA	0.5	1	0.25	50	9	0	3
	Liu et al. [49]	2016	140.88	NA	0.86	0.74	31	6	5	17
	Bokacheva et al. [50]	2014	0.58	0.84	0.85	0.86	22	2	4	12
F	Meng et al. [40]	2020	4.99	0.766	0.7385	0.7586	48	14	17	44
	Zhao et al. [43]	2018	20.3	0.885	0.857	0.893	50	2	17	20
	Xijin Mao [44]	2018	7.86	0.601	64.9	57.4	NA	NA	NA	NA
	Lin et al. [45]	2017	7.87	0.802	0.863	0.66	44	16	7	31
	Cho et al. [47]	2015	NA	0.72	0.833	0.726	42	3	8	9
	Liu et al. [49]	2016	7.2	NA	0.86	0.74	31	6	5	17
	Bokacheva et al. [50]	2014	4.9	0.79	0.73	0.86	19	2	7	12

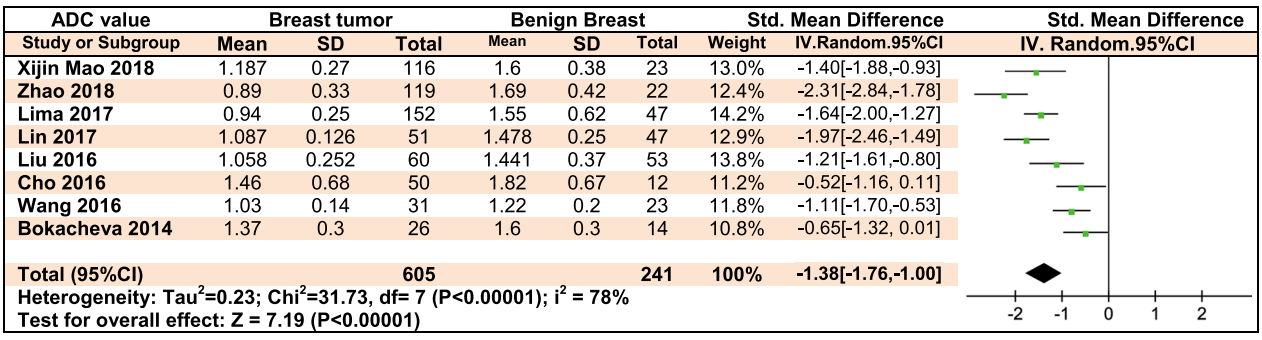

Fig. 2 The mean value of the apparent diffusion coefficient (ADC) distinguished among breast lesions

0.575–0.908). The optimal cutoff of *D* during the NAC to differentiate pCR from non-pCR was 0.971×10^{-3}mm^2/s, which showed a sensitivity of 100% (95% CI 66.4%–100%) and a specificity of 63.2% (95% CI 38.4%–83.7%). At the beginning of the follow-up, Kim et al. [36] recommended the administration of IVIM-DW imaging factors of good and minor responders pre and post NAC. Prior to NAC, while Dmean was lower in poor responders versus good

D value	Breast tumor			Benign Breast			Std. Mean Difference	Std. Mean Difference
Study or Subgroup	Mean	SD	Total	Mean	SD	Total	Weight	IV.Random.95%CI
Meng 2020	0.93	0.32	65	1.32	0.29	58	11.8%	-1.17[-1.55,-0.78]
Xijin Mao 2018	0.86	0.33	116	1.3	0.46	23	11.0%	-1.24[-1.71,-0.76]
Zhao 2018	0.75	0.38	119	1.51	0.31	22	10.6%	-2.04[-2.56,-1.53]
Chen WJ 2017	0.873	0.225	18	1.437	0.53	11	7.4%	-1.63[-2.50,-0.75]
Ma 2017	0.99	0.22	81	1.34	0.17	47	11.5%	-1.71[-2.13,-1.29]
Lin 2017	0.931	0.129	51	1.398	0.29	47	10.8%	-2.06[-2.55,-1.56]
Liu 2016	0.85	0.5	36	1.23	0.5	23	10.3%	-0.75[-1.29,-0.21]
Cho 2016	1.35	0.65	50	1.89	0.7	12	9.3%	-0.85[-1.50,-0.20]
Wang 2016	0.91	0.15	31	1.32	0.15	23	8.4%	-2.69[-3.45,-1.94]
Bokacheva 2014	1.28	0.28	26	1.56	0.28	14	9.0%	-0.95[-1.63,-0.26]
Total (95%CI)			593			280	100%	-1.50[-1.85,-1.14]
Heterogeneity: Tau^2=0.24; Chi^2=37.49, df= 9 (P<0.00001); i^2 = 76%								
Test for overall effect: Z = 8.33 (P<0.00001)								

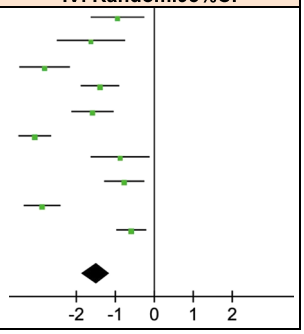

Fig. 3 The mean value of the true diffusivity (*D*) distinguished among breast lesions

D* value	Breast tumor			Benign Breast			Std. Mean Difference	Std. Mean Difference
Study or Subgroup	Mean	SD	Total	Mean	SD	Total	Weight	IV.Random.95%CI
Muzhen He 2021	15.25	12.19	18	12.02	3.19	11	7.4%	0.32[-0.44, 1.07]
Meng 2020	31.12	8.23	65	27.04	7.11	58	8.8%	0.53[0.16, 0.89]
Xijin Mao 2018	3.85	5.18	116	3.07	4.9	23	8.5%	0.15[-0.30, 0.60]
Zhao 2018	41.01	20.63	119	54.2	21.2	22	8.5%	-0.63[-1.09,-0.17]
Jiang 2017	63.7	44.9	31	52.5	46.2	35	8.4%	0.24[-0.24, 0.73]
Ma 2017	7.64	2.07	81	6.83	2.13	47	8.8%	0.38[0.02, 0.75]
Lima 2017	13.6	19.9	152	100	90.6	47	8.8%	-1.83[-2.2,-1.45]
Lin 2017	101.20	29.01	51	126.04	40.9	47	8.7%	-0.7[-1.11,-0.29]
Liu 2016	109.75	50	36	155.2	50	23	8.2%	-0.9[-1.45,-0.35]
Cho 2016	17.73	4.45	50	18.03	16.5	12	7.9%	-0.04[-0.67,0.59]
Wang 2016	26.54	21.91	31	45.46	25.2	23	8.2%	-0.8[-1.36,-0.24]
Bokacheva 2014	21.7	11	26	27.6	34	14	7.8%	-0.27[-0.92,0.39]
Total (95%CI)			776			362	100%	-0.30[-0.76,0.16]
Heterogeneity: Tau^2=0.58; Chi^2=123.02, df= 11 (P<0.00001); i^2 = 91%								
Test for overall effect: Z = 1.29 (P = 0.20)								

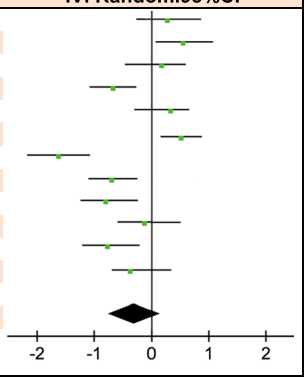

Fig. 4 The mean value of the pseudo-diffusivity (*D**) distinguished among breast lesions

f value	Breast tumor			Benign Breast			Std. Mean Difference	Std. Mean Difference
Study or Subgroup	Mean	SD	Total	Mean	SD	Total	Weight	IV.Fixed.95%CI
Meng 2020	5.45	1.46	65	3.96	1.72	58	13.3%	0.93[0.56, 1.31]
Xijin Mao 2018	9.33	5.18	116	7.15	6.87	23	9.1%	0.4[-0.05, 0.84]
Zhao 2018	33.05	11.53	119	17.76	7.74	22	7.9%	1.38[0.89, 1.86]
Chen WJ 2017	10.63	3.44	18	7.86	3.7	11	3.0	0.79[0.01, 1.57]
Jiang 2017	6.3	2.1	31	3.88	2.06	35	6.7%	1.15[0.63,1.67]
Ma 2017	8.53	2.14	81	7.68	1.97	47	14.0%	0.41[0.04, 0.77]
Lima 2017	5.14	4.42	152	0.76	3.8	47	15.8%	1.02[0.68, 1.36]
Lin 2017	10.22	2.764	51	6.402	3.63	47	10.0%	1.18[0.75, 1.61]
Liu 2016	10.23	5	36	5.34	3	23	5.8%	1.11[0.55,1.68]
Cho 2016	9.4	5.1	50	5	3	12	4.4%	0.85[0.20, 1.49]
Wang 2016	21.18	7.84	31	15.16	9.9	23	6.0%	0.68[0.12, 1.23]
Bokacheva 2014	6.5	3.1	26	3.1	3.3	14	3.9%	1.02[0.33, 1.71]
Total (95%CI)			776			362	100%	0.89[0.75,1.02]
Heterogeneity: Chi^2=20.07, df= 11 (P=0.04); i^2 = 45%								
Test for overall effect: Z = 12.8 (P<0.00001)								

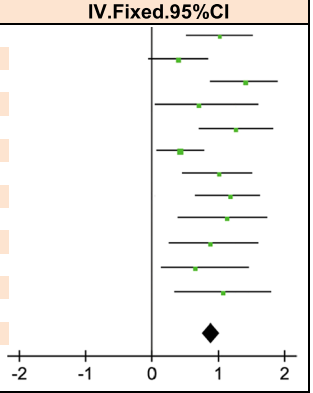

Fig. 5 The mean value of the perfusion volume fraction (*f*) distinguished among breast lesions

responders ($P \leq 0.043$). After NAC, Dmean, was lower in poor responders ($P \leq 0.037$). We found no difference between the study groups concerning D^* and f values both prior to and following NAC ($P \geq 0.07$). While in Cho et al. [37] the values of average Dt of responders were lower than before NAC was 0.99 (0.55, 2.16) μm^2/ms, the average values *fp* and *Dp* for responders were 8.7 (4.8, 19.3)% and 25.54 (15.99, 37.14) μm^2/ms while 1.05 (0.96,

Table 4 The pooled estimation of sensitivity and specificity of breast lesions

Indicators	Sensitivity	Specificity	AUC	I^2	
				Sensitivity %	Specificity %
ADC	0.76 (0.65, 0.85)	0.79 (0.68, 0.87)	0.85 (0.81, 0.87)	76.66	38.87
D	0.86 (0.77, 0.91)	0.86 (0.80, 0.90)	0.91 (0.88, 0.93)	79.59	19.14
*D**	0.84 (0.66, 0.94)	0.59 (0.47, 0.70)	0.71 (0.67, 0.75)	79.84	61.72
f	0.80 (0.74, 0.85)	0.76 (0.68, 0.83)	0.85 (0.82, 0.88)	15.09	16.32

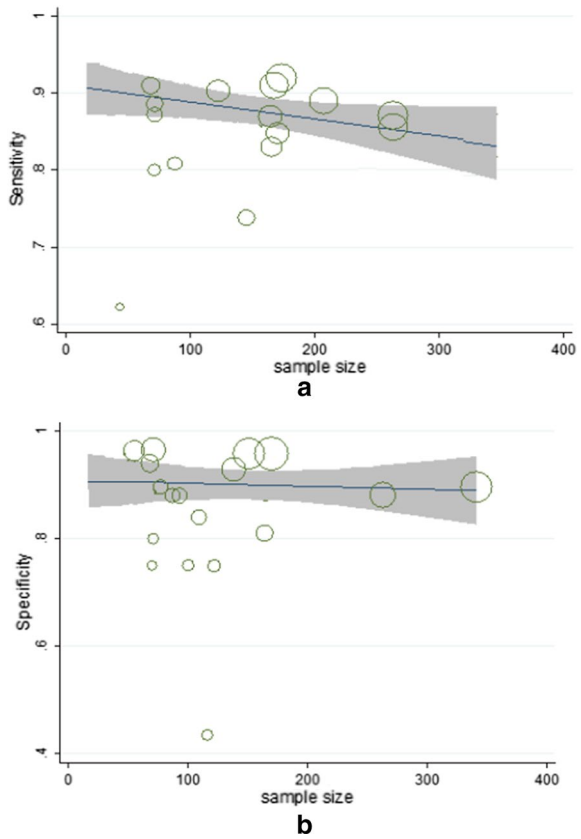

Fig. 6 The distribution of estimated sensitivity (**a**) and specificity (**b**) according to different sample sizes

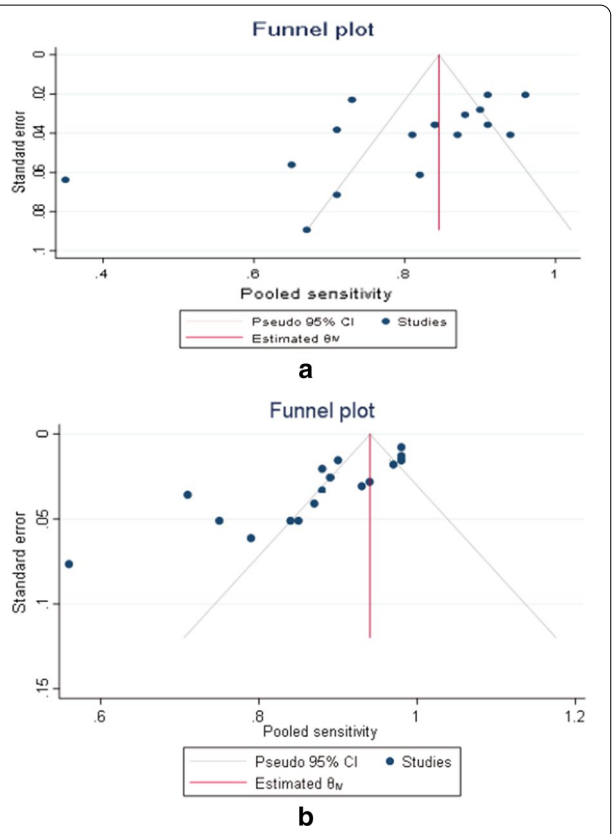

Fig. 7 The funnel plot to assess publication bias in estimated sensitivity (**a**) and specificity (**b**)

1.21) μm^2/ms, 11.7 (5.2, 14.2)%, and 17.16 (16.9, 25.79) μm^2/ms for nonresponders. The results for all parameters are summarized in Table 4.

Discussion

Individual patients and treatment regimens might have a wide range of responses to NAC. Breast MRI could be a useful imaging tool for determining whether there are changes in MRI parameters between (histopathological) responders and nonresponders before and after treatment. Intravoxel incoherent motion imaging can quantify both real molecular diffusion and motion of water molecules in the capillary network using a single diffusion-weighted acquisition technique. Utilizing the IVIM imaging model and numerous b values, IVIM imaging is used to reflect tissue diffusivity and microcapillary perfusion, as opposed to standard DWI using a pair of b values. Biexponential IVIM imaging modeling can yield three parameters, like *D*, the diffusion-related parameter (that shows the true molecular diffusion of the nonvascular compartment related to Brown movement)t; *D**, the pseudo-diffusion coefficient (that macroscopically shows the incoherent movement of blood in the microvascular

compartment); and *f*, the perfusion fraction (that shows the percentage of incoherent signal due to the vascular compartment in each voxel as a proportion of the total incoherent signal) [23]. Furthermore, tumor diameter and volume cannot be used to distinguish chemotherapy final responders and nonresponders. Several studies, on the other hand, revealed significant alternations in diameter and/or volume of the tumor following the initial cycle of NAC, which can be used to differentiate between patient groups.

In our study, the SMDs proposed breast tumors confirmed ADC and *D* lower values and *f* values higher than did benign lesions. BC usually has dense cellularity with a high ability for propagation, which may decrease the extracellular space and boundary the diffusion of water molecules thus causing a reduction in the diffusion coefficient.

Captivatingly, breast tumors proved a significantly greater *f* value but a nonsignificantly greater *D** value than the benign tissue. This mostly arose from improved angiogenesis in BC [14]. The *f* value also confirmed a greater specificity of 0.76 and an AUC of 0.85 related with the specificity of 0.59 and AUC of 0.71 for the *D** value.

Kim et al. [36], for example, proved the mean, 25th, 50th, and 75th percentiles of ADC and *D* enhanced in the total study group after two cycles of NAC, which might indicate reduced cellularity owing to treatment effects. The majority of these variables were likewise related to NAC response. These findings support earlier findings that good vs poor responders had considerably greater post-NAC ADC or *D* values [38, 51]. Meanwhile, in the entire trial population, *D** and *f* values did not change substantially before and after NAC and were not effective for predicting tumor response. Unlike ADC and *D*, which have reduced signal attenuation fluctuation, D* and *f* have poor measurement repeatability [52, 53]. According to Che et al., significant swings in *D** values may overpower minor alternations in *D** [38]. Intratumoral heterogeneity and noise fluctuations might potentially have an impact on the outcomes [52]. To improve repeatability, more research should be conducted.

In addition, Cho et al. found that in their pathologic complete response (pCR) group, the post-NAC *f* value was significantly lower [37]. They reported a negative association between microvascular structures and *f* value in good responders. Nevertheless, we did not find significant results in *f* values to predict therapy response. In contrast to the other DW parameters, *f* values exhibited very poor inter-observer agreement, with a large range of values across the cases. No study used the *f* values to evaluate chemo-radiation therapy response in breast cancer patients [54]. In this context, Kim et al. [36] found that pre-NAC D_{mean}, D50, and D75 were significantly lower in poor responders. There are controversies regarding the administration of DW imaging parameters as pretreatment predictors for pathologic response. Some studies reported that ow pre-NAC ADC or *D* tends to respond better to NAC in BC [39, 55]; however, some also reported no difference in pre-NAC ADC or *D* between pCR and non-pCR groups [16, 17]. There are studies that found differences in the predictive value of pre-NACADC based on the subtypes of BC [56]. The findings revealed no difference concerning other pre-NAC DW values, i.e., ADC, *D**, or *f*, between good and minor responders. We found that good responders tended to have higher changes in ADC and *D* values, which was not statistically significant. Some articles found a significantly higher lower in ADC or *D* in nonresponders compared to responders [38, 39].

Cho et al. [37] reported that particular IVIM factors could differentiate between RECIST responders and nonresponders. Initial measurements revealed that Dp and VTT% had the highest level of prognosis, as high vascularity with slow and heterogeneous pseudo-diffusion offering poor prognosis; in the same vein, for all dual-scanned responders, Dp was decreased. Furthermore, the heterogeneity metrics of Dp revealed surprising findings and showed the administration of advanced metrics within IVIM analysis. Histogram investigation presented the potential to detect dissimilarities in tumor heterogeneity between the two groups. The findings regarding Dp and VTT% showed that the vascular entities from lesions can have a potential role to predict the response to NAT, and heterogeneity in the distribution of blood volume may be an optimal parameter to predict the response. Recently conducted studies on cancer patients showed IVIM differences between responders and nonresponders [38, 54], indicating the potential predicting role of vascular, along with cellular, IVIM parameters [38].

Che et al. [38] reported that an increased level of *D* following 2 cycles of NAC in cases under tumor treatment may indicate decreased cellularity because of necrosis and fibrotic alternation caused by the treatment, which is consistent with some of the previous studies [44, 57]. We found a significant decline in the *f* value of all subjects during the treatment. Following chemotherapy, consumption of cytotoxic drugs causes apoptosis of tumor cells, which in turn led to decreased cell density and immature endothelial cells; the extracellular spaces will expand that fades the restrictions for water molecules movement and weakening the process of perfusion [58, 59]. In a study, Liu et al. [49] reported insignificant association *D** values with reason the depressed SNR ratio and the low measure reproducibility. Xiao and colleagues [59] found a significantly higher *D* and lower *D** value following NAC in nasopharyngeal cancer; however,

they reported a *f* value that is more consistent. According to the findings, *D* value was significantly higher and lower, respectively, following NAC, which is in line with the study by Li et al. [60]. Nevertheless, there was no significant difference concerning the decrease of *D** [61].

Chemotherapy's cytotoxic and anti-angiogenic effects may cause tumor cell and microvessel density to decrease. On the one hand, the cytotoxic impact of chemotherapeutic drugs causes an excessive amount of micro necrosis in tumor cells. Because of the larger extracellular and extravascular gaps, pure water diffusion motion becomes more unconstrained, increasing the *D* value. As a result of the improved chemotherapeutic response to NAC, the *D* value has significantly increased. The *f* value, on the other hand, is primarily linked to the volume fraction of microcirculation [61]. In breast cancers, successful chemotherapy causes death of cytotoxic tumors, which in turn led to a reduction of the proportion of immature microvessel density [62].

As a result, microvascular structures would diminish more significantly, resulting in a higher *f* value and a greater chemotherapeutic response to NAC. Simultaneously, the pCR group patients showed a trend toward a larger change in *D** value, though the two groups were not significantly different. These findings imply that changes in IVIM-MRI characteristics can be applied for the prediction of chemotherapeutic responsiveness in cases with BC at an early stage of NAC. The link between parameter values and NAC effects, as measured by mass shrinkage, thus supports the usefulness of IVIM parameters to forecast and monitor events early. Middle treatment *D* and change of *D* and *f* measurements were found to be the most sensitive to mass shrinking among pre- and mid-treatment, and change of *D* and *f* evaluations, but pretreatment *D* exhibited no statistically significant link with mass shrinkage.

Our study had some flaws that needed to be addressed. First, evaluate the small number of IVIM-DWI studies that have been reported in the same patient group. Second, the majority of studies have a small sample size, and the bulk of them are single-center research. If sample sizes are expanded in (future) multi-center research to determine the genuine precision of MRI in the NAC scenario with higher confidence, statistical noise will be reduced. Third, we were unable to conduct a meta-analysis because of the heterogeneity among studies, which could be due to the diverse types and stages of breast cancer. As a result, rather than completing a meta-analysis that employs statistical models to address such heterogeneities to some extent, the research team decided to conduct a systematic review to develop a descriptive presentation. Finally, we admit that there are additional potential limitations, such as selector bias, which was caused by the research selection, publication, and verification.

Conclusions

The estimated sensitivity and specificity in the current meta-analysis were acceptable, so can help radiologists achieve the needed sensitivity and specificity, while also ensuring consistent reporting and communication between radiologists and other physicians within an institution, between different institutions, and worldwide.

During cancer therapy, these techniques can give useful clinical, noninvasive biomarkers. We show that various IVIM indicators have the potential to be used as predictors of NAT treatment response, as well as spatially dependent physiological alterations that occur after therapy. Also the results of this review confirmed that the IVIM conclusion is significantly superior in malignant breast tissues than in benign tissues also normal breast, and the IVIM parameters may advance the accuracy of breast tumors differentiation from tumors tissues. In the advanced breast, IVIM-derived metrics, particularly the *D* and *f* values, had a major contribution to the evaluation, pre-treatment prognosis, and monitoring of early responses to NAC. Patients with lower baseline *D* value and a high *f* value were found to respond better to neoadjuvant chemotherapy after treatment. The present overall studies showed that the parameters *D* and *f* were more reliable predictors of pretreatment in pathological response than the other parameters, the *D* value was significantly higher in the pCR than that in the non-pCR and also described that as the microvascular structures decrease more in the pCR, a greater decrease in the *f*-value might be observed. The IVIM model's *D* and *f* values suggested that they could be administered for early therapy prediction and monitoring the response. More research is needed to confirm the IVIM biomarkers' predictive utility in longitudinal BC research for both therapy and outcome monitoring.

Abbreviations

ADC: Apparent diffusion coefficient; BC: Breast cancer; *D**: Pseudo-diffusivity; *D*: Tissue diffusivity; DTI: Diffusion tensor imaging; DWMRI: Diffusion-weighted magnetic resonance imaging; *f*: Perfusion volume fraction; IVIM: Intravoxel incoherent motion; MRI: Magnetic resonance imaging.

Acknowledgements

None.

Author contributions

M.S, A.A, and N.A contributed to study concept and design; M.S, R.A, and H.D collected the data; A.A and N.A carried out analysis and interpretation of data; M.S performed drafting of the manuscript; M.S, R.A, and H.D performed critical revision of the manuscript for important intellectual content. All authors read and approved the final manuscript.

Funding
The authors state that this work has not received any funding.

Availability of data and material
Not applicable.

Declarations

Ethics approval and consent to participate
Ethical approval will not be required since this study will be based on published data.

Consent for publication
Not applicable.

Competing interests
The authors have no conflicts of interest to disclose.

Author details
[1]Department of Technology of Radiology and Radiotherapy, International Campus, Tehran University of Medical Sciences (TUMS), Tehran, Iran. [2]Radiology-TUMS (Cancer Institute-ADIR), Tehran University of Medical Sciences (TUMS), Tehran, Iran. [3]Radiology-Medical Imaging Center, Cancer Research Institute, Imam Khomeini Hospital Advanced Diagnostic and Interventional Radiology Research Center (ADIR), Tehran University of Medical Sciences (TUMS), Tehran, Iran.

Received: 25 January 2022 Accepted: 10 April 2022
Published online: 26 April 2022

References

1. Voduc KD, Cheang MC, Tyldesley S, Gelmon K, Nielsen TO, Kennecke H (2010) Breast cancer subtypes and the risk of local and regional relapse. J Clin Oncol 28:1684–1691
2. Ades F, Zardavas D, Bozovic-Spasojevic I, Pugliano L, Fumagalli D, de Azambuja E, Viale G, Sotiriou C, Piccart M (2014) Luminal B breast cancer: molecular characterization, clinical management, and future perspectives. J Clin Oncol 32:2794–2803
3. Cheang MC, Chia SK, Voduc D, Gao D, Leung S, Snider J, Watson M, Davies S, Bernard PS, Parker JS et al (2009) Ki67 index, HER2 status, and prognosis of patients with luminal B breast cancer. J Natl Cancer Inst 101:736–750
4. Goldhirsch A, Wood WC, Coates AS, Gelber RD, Thürlimann B (2011) Senn HJ and Panel members: Strategies for subtypes-dealing with the diversity of breast cancer: highlights of the St. Gallen international expert consensus on the primary therapy of early breast cancer 2011. Ann Oncol 22:1736–1747
5. Goldhirsch A, Winer EP, Coates AS, Gelber RD, Piccart-Gebhart M, Thürlimann B (2013) Senn HJ and Panel members: Personalizing the treatment of women with early breast cancer: highlights of the St. Gallen international expert consensus on the primary therapy of early breast cancer 2013. Ann Oncol 24:2206–2223
6. Boisserie-Lacroix M, Hurtevent-Labrot G, Ferron S, Lippa N, Bonnefoi H, Mac Grogan G (2013) Correlation between imaging and molecular classification of breast cancers. Diagn Interv Imaging 94:1069–1080
7. Mazurowski MA, Zhang J, Grimm LJ, Yoon SC, Silber JI (2014) Radiogenomic analysis of breast cancer: luminal B molecular subtype is associated with enhancement dynamics at MR imaging. Radiology 273:365–372
8. Aberle DR, Chiles C, Gatsonis C, Hillman BJ, Johnson CD, McClennan BL, Mitchell DG, Pisano ED, Schnall MD, Sorensen AG (2005) American College of Radiology Imaging Network: imaging and cancer: research strategy of the American college of radiology imaging network. Radiology 235:741–751
9. Zhang L, Li J, Xiao Y, Cui H, Du G, Wang Y, Li Z, Wu T, Li X, Tian J (2015) Identifying ultrasound and clinical features of breast cancer molecular subtypes by ensemble decision. Sci Rep 5:11085
10. Brandao AC, Lehman CD, Partridge SC (2013) Breast magnetic resonance imaging: diffusion-weighted imaging. Magn Reson Imaging Clin N Am 21:321–336
11. Padhani AR, Liu G, Koh DM, Chenevert TL, Thoeny HC, Takahara T, Dzik-Jurasz A, Ross BD, Van Cauteren M, Collins D et al (2009) Diffusion-weighted magnetic resonance imaging as a cancer biomarker: consensus and recommendations. Neoplasia 11:102–125
12. Basser PJ (1995) Inferring microstructural features and the physiological state of tissues from diffusion-weighted images. NMR Biomed 8:333–344
13. Woodhams R, Ramadan S, Stanwell P, Sakamoto S, Hata H, Ozaki M, Kan S, Inoue Y (2011) Diffusion-weighted imaging of the breast: principles and clinical applications. Radiographics 31:1059–1084
14. Atuegwu NC, Arlinghaus LR, Li X, Welch EB, Chakravarthy BA, Gore JC, Yankeelov TE (2011) Integration of diffusion-weighted MRI data and a simple mathematical model to predict breast tumor cellularity during neoadjuvant chemotherapy. Magn Reson Med 66:1689–1696
15. Yoshikawa MI, Ohsumi S, Sugata S, Kataoka M, Takashima S, Mochizuki T, Ikura H, Imai Y (2008) Relation between cancer cellularity and apparent diffusion coefficient values using diffusion-weighted magnetic resonance imaging in breast cancer. Radiat Med 26:222–226
16. Squillaci E, Manenti G, Di Roma M, Miano R, Palmieri G, Simonetti G (2004) Correlation of diffusion-weighted MR imaging with cellularity of renal tumours. Anticancer Res 24:4175–4179
17. Partridge SC, DeMartini WB, Kurland BF, Eby PR, White SW, Lehman CD (2009) Quantitative diffusion-weighted imaging as an adjunct to conventional breast MRI for improved positive predictive value. AJR Am J Roentgenol 193:1716–1722
18. Sinha S, Lucas-Quesada FA, Sinha U, DeBruhl N, Bassett LW (2002) In vivo diffusion-weighted MRI of the breast: potential for lesion characterization. J Magn Reson Imaging 15:693–704
19. Fornasa F, Pinali L, Gasparini A, Toniolli E, Montemezzi S (2011) Diffusion-weighted magnetic resonance imaging in focal breast lesions: analysis of 78 cases with pathological correlation. Radiol Med 116:264–275
20. Malayeri AA, El Khouli RH, Zaheer A, Jacobs MA, Corona-Villalobos CP, Kamel IR, Macura KJ (2011) Principles and applications of diffusion weighted imaging in cancer detection, staging, and treatment follow-up. Radiographics 31:1773–1791
21. Le Bihan D, Breton E, Lallemand D, Grenier P, Cabanis E, Laval-Jeantet M (1986) MR imaging of intravoxel incoherent motions: application to diffusion and perfusion in neurologic disorders. Radiology 161:401–407
22. Koh DM, Collins DJ, Orton MR (2011) Intravoxel incoherent motion in body diffusion weighted MRI: reality and challenges. AJR Am J Roentgenol 196:1351–1361
23. Le Bihan D, Breton E, Lallemand D, Aubin ML, Vignaud J, Laval-Jeantet M (1988) Separation of diffusion and perfusion in intravoxel incoherent motion MR imaging. Radiology 168:497–505
24. Suo S, Lin N, Wang H, Zhang L, Wang R, Zhang S, Hua J, Xu J (2015) Intravoxel incoherent motion diffusion-weighted MR imaging of breast cancer at 3.0 tesla: comparison of different curve-fitting methods. J Magn Reson Imaging 42:362–370
25. Kim Y, Ko K, Kim D, Min C, Kim SG, Joo J, Park B (2016) Intravoxel incoherent motion diffusion-weighted MR imaging of breast cancer: association with histopathological features and subtypes. Br J Radiol 89:20160140
26. Sigmund EE, Cho GY, Kim S, Finn M, Moccaldi M, Jensen JH, Sodickson DK, Goldberg JD, Formenti S, Moy L (2011) Intravoxel incoherent motion imaging of tumor microenvironment in locally advanced breast cancer. Magn Reson Med 65:1437–1447
27. Meacham CE, Morrison SJ (2013) Tumour heterogeneity and cancercell plasticity. Nature 501:328–337
28. Fisher R, Pusztai L, Swanton C (2013) Cancer heterogeneity: implications for targeted therapeutics. Br J Cancer 108:479–485
29. Polyak K (2011) Heterogeneity in breast cancer. J Clin Invest 121:3786–3788
30. Iima M, Yano K, Kataoka M, Umehana M, Murata K, Kanao S, Togashi K, Le Bihan D (2015) Quantitative non-gaussian diffusion and intravoxel incoherent motion magnetic resonance imaging: differentiation of malignant and benign breast lesions. Invest Radiol 50:205–211
31. Liu C, Liang C, Liu Z, Zhang S, Huang B (2013) Intravoxel incoherent motion (IVIM) in evaluation of breast lesions: comparison with conventional DWI. Eur J Radiol 82:e782–e789

32. Cho GY, Moy L, Kim SG, Baete SH, Moccaldi M, Babb JS, Sodickson DK, Sigmund EE (2016) Evaluation of breast cancer using intravoxel incoherent motion (IVIM) histogram analysis: comparison with malignant status, histological subtype, and molecular prognostic factors. Eur Radiol 26:2547–2558
33. Alili C, Pages E, Curros Doyon F, Perrochia H, Millet I, Taourel P (2014) Correlation between MR imaging-prognosis factors and molecular classification of breast cancers. Diagn Interv Imag 95:235–242
34. Uematsu T, Kasami M, Yuen S (2009) Triple-negative breast cancer: correlation between MR imaging and pathologic findings. Radiology 250:638–647
35. Suo S, Yin Y, Geng X, Zhang D, Hua J, et al. Diffusion-weighted MRI for predicting pathologic response to neoadjuvant chemotherapy in breast cancer: evaluation with mono-, bi-, and stretched-exponential models. 2021; 19:236.
36. Kim Y, Kim SH, Lee HW, Song BJ, Kang BJ, Lee A et al (2018) Intravoxel incoherent motion diffusion-weighted MRI for predicting response to neoadjuvant chemotherapy in breast cancer. Magn Reson Imaging 48:27–33
37. Cho GY, Gennaro L, Sutton EJ, Zabor EC, Zhang Z, Giri D et al (2017) Intravoxel incoherent motion (IVIM) histogram biomarkers for prediction of neoadjuvant treatment response in breast cancer patients. Eur J Radiol Open 4:101–107
38. Che S, Zhao X, Yanghan O, Li J, Wang M, Wu B et al (2016) Role of the intravoxel incoherent motion diffusion weighted imaging in the pretreatment prediction and early response monitoring to neoadjuvant chemotherapy in locally advanced breast cancer. Medicine 95(4):66
39. Bedair R, Priest AN, Patterson AJ, McLean MA, Graves MJ, Manavaki R et al (2017) Assessment of early treatment response to neoadjuvant chemotherapy in breast cancer using non-mono-exponential diffusion models: a feasibility study comparing the baseline and mid-treatment MRI examinations. Eur Radiol 27(7):2726–2736
40. He M et al (2021) Application of diffusion weighted imaging techniques for differentiating benign and malignant breast lesions. Front Oncol 11:2422
41. Meng N, Wang XJ, Sun J, Huang L, Wang Z, Wang KY et al (2020) Comparative study of amide proton transfer-weighted imaging and intravoxel incoherent motion imaging in breast cancer diagnosis and evaluation. J Magn ResonImaging 52:1175–1186
42. Song SE, Cho KR, Seo BK, Woo OH, Park KH, Son YH et al (2019) Intravoxel incoherent motion diffusion-weighted MRI of invasive breast cancer: correlation with prognostic factors and kinetic features acquired with computer-aided diagnosis. J Magn Reson Imaging 49:118–130
43. Zhao M, Fu K, Zhang L, Guo W, Wu Q, Bai X et al (2018) Intravoxel incoherent motion magnetic resonance imaging for breast cancer: a comparison with benign lesions and evaluation of heterogeneity in different tumor regions with prognostic factors and molecular classification. Oncol Lett 16:5100–5112
44 Mao X et al (2018) Quantitative evaluation of intravoxel incoherent motion diffusion-weighted imaging (IVIM) for differential diagnosis and grading prediction of benign and malignant breast lesions. Medicine 97:26
45. Lin N, Chen J, Hua J, Zhao J, Zhao J, Lu J (2017) Intravoxel incoherent motion MR imaging in breast cancer: quantitative analysis for characterizing lesions. Int J Clin Exp Med 10:1705–1714
46. Iima M, Kataoka M, Kanao S, Onishi N, Kawai M, Ohashi A et al (2018) Intravoxel incoherent motion and quantitative non-gaussian diffusion MR Imaging: evaluation of the diagnostic and prognostic value of several markers of malignant and benign breast lesions. Radiology 287:432–441
47. Cho GY, Moy L, Kim SG, Baete SH, Moccaldi M, Babb JS et al (2016) Evaluation of breast cancer using intravoxel incoherent motion (IVIM) histogram analysis: comparison with malignant status, histological subtype, and molecular prognostic factors. Eur Radiol 26:2547–2558
48. Wang Q, Guo Y, Zhang J, Wang Z, Huang M, Zhang Y (2016) Contribution of IVIM to conventional dynamic contrast-enhanced and diffusion-weighted MRI in differentiating benign from malignant breast masses. Breast Care 11:254–258
49. Liu C, Wang K, Chan Q, Liu Z, Zhang J, He H et al (2016) Intravoxel incoherent motion MR imaging for breast lesions: comparison and correlation with pharmacokinetic evaluation from dynamic contrast-enhanced MR imaging. Eur Radiol 26:3888–3898
50. Bokacheva L, Kaplan JB, Giri DD, Patil S, Gnanasigamani M, Nyman CG et al (2014) Intravoxel incoherent motion diffusion-weighted MRI at 3.0 T differentiates malignant breast lesions from benign lesions and breast parenchyma. J Magn Reson Imaging 40:813–23
51. Fangberget A, Nilsen L, Hole KH, Holmen M, Engebraaten O, Naume B et al (2011) Neoadjuvant chemotherapy in breast cancer-response evaluation and prediction of response to treatment using dynamic contrast-enhanced and diffusion-weighted MR imaging. Eur Radiol 21(6):1188–1199
52. Andreou A, Koh D, Collins D, Blackledge M, Wallace T, Leach M et al (2013) Measurement reproducibility of perfusion fraction and pseudodiffusion coefficient derived by intravoxel incoherent motion diffusion-weighted MR imaging in normal liver and metastases. Eur Radiol 23(2):428–434
53 Kakite S, Dyvorne H, Besa C, Cooper N, Facciuto M, Donnerhack C et al (2015) Hepatocellular carcinoma: Short-term reproducibility of apparent diffusion coefficient and intravoxel incoherent motion parameters at 30 T. J Magn Resonan Imaging 41(1):149–56
54. Nougaret S, Vargas HA, Lakhman Y, Sudre R, Do RK, Bibeau F et al (2016) Intravoxel incoherent motion–derived histogram metrics for assessment of response after combined chemotherapy and radiation therapy in rectal cancer: initial experience and comparison between single-section and volumetric analyses. Radiology 280(2):446–454
55. Park SH, Moon WK, Cho N, Song IC, Chang JM, Park I-A et al (2010) Diffusion-weighted MR imaging: pretreatment prediction of response to neoadjuvant chemotherapy in patients with breast cancer. Radiology 257(1):56–63
56. Partridge SC, Nissan N, Rahbar H, Kitsch AE, Sigmund EE (2017) Diffusion-weighted breast MRI: clinical applications and emerging techniques. J Magn Reson Imaging 45(2):337–355
57. Fujimoto H, Kazama T, Nagashima T, Sakakibara M, Suzuki TH, Okubo Y et al (2014) Diffusion-weighted imaging reflects pathological therapeutic response and relapse in breast cancer. Breast Cancer 21(6):724–731
58. Ah-See M-LW, Makris A, Taylor NJ, Harrison M, Richman PI, Burcombe RJ et al (2008) Early changes in functional dynamic magnetic resonance imaging predict for pathologic response to neoadjuvant chemotherapy in primary breast cancer. Clin Cancer Res 14(20):6580–9
59 Xiao Y, Pan J, Chen Y, Chen Y, He Z, Zheng X (2015) Intravoxel incoherent motion-magnetic resonance imaging as an early predictor of treatment response to neoadjuvant chemotherapy in locoregionally advanced nasopharyngeal carcinoma. Medicine 94(24):66
60. Li XR, Cheng LQ, Liu M, Zhang YJ, Wang JD, Zhang AL, Song X, Li J, Zheng YQ, Liu L (2012) DW-MRI ADC values can predict treatment response in patients with locally advanced breast cancer undergoing neoadjuvant chemotherapy. Med Oncol 29(2):425–431
61. Rastogi P, Anderson SJ, Bear HD, Geyer CE, Kahlenberg MS, Robidoux A et al (2008) Preoperative chemotherapy: updates of national surgical adjuvant breast and bowel project protocols B-18 and B-27. J Clin Oncol 26(5):778–785
62. Darland DC, D'Amore PA (1999) Blood vessel maturation: vascular development comes of age. J Clin Investig 103(2):157–158
63. Whiting PF, Rutjes AW, Westwood ME, Mallett S, Deeks JJ, Reitsma JB et al (2011) QUADAS-2: a revised tool for the quality assessment of diagnostic accuracy studies. Ann Intern Med 155(8):529–536

Publisher's Note